

# High plasmon concentration on the surfaces of rectangular metallic rods embedded in air in a 2D photonic crystal

D. M. Calvo-Velasco<sup>1</sup> · N. Porrás-Montenegro<sup>1</sup>

Received: 20 August 2015 / Accepted: 14 November 2015 / Published online: 21 March 2016  
© Springer-Verlag Berlin Heidelberg 2016

**Abstract** Using the revised plane wave method, we calculated the photonic band structure (PBS) considering TE polarization of a square 2D photonic crystal made of rectangular metallic rods embedded in air. In case of square rods and comparing different plasma frequencies, we found a characteristic band distribution related with the existence of localized plasmons on the rod surfaces, and also we found that this type of rod shape contributes to a high concentration of the electromagnetic field close to the rod corners. Considering rectangular rods and varying one of the sides of the rods, we found a PBS that presents a reorganization of the bands in comparing with the low dispersion present in the square rod case, related with a high localization of the radiation on the rod surfaces.

## 1 Introduction

In the last decades the study of photonic crystals (PCs) and their optical properties [1–3], aroused the interest of the scientific community, thanks to the discovery of the photonic band gaps present in these structures, that is, frequency ranges where the propagation of the electromagnetic field is prohibited, allowing the development of new technologies [4].

PCs are arrangements of materials with different refraction index, which allow light behaviors not present in the bulk materials that form the PC. The photonic band structure (PBS) and the band gaps in the PCs depend on the

difference between the refractive index of the components of the PC, their geometry disposition, and the filling fraction. The different studies on these structures vary from multiple slabs of different materials for 1D systems up to 3D structures [1–8], including fractal disposition of a dielectric material in air in a limited region of the space [9, 10]. Also, some studies are related to defects which modify the translation symmetry of PCs which allows the existence of high localized modes used in the construction of wave guides [11, 12].

Maxwell equations are used to study the light behavior in PCs. To solve them several techniques have been developed such as plane waves, finite difference time domain (FDTD), revised plane wave method (RPWM), and others [13], and have been applied to several systems in order to study their optical response [14, 17, 18].

For PCs formed by dispersive materials, it is possible to locate the incident radiation thanks to the existence of surface plasmon polaritons, that are related with the collective motion of coupled charges with the electromagnetic field [19].

Kusmiak et al. [14] studied a 2D system made of an array of parallel metallic rods in air using the plane wave method, reducing the PBS calculation to a standard eigenvalue problem. They showed the existences of localized modes for TE polarization that must correspond to the interaction of the rod isolated excitations that overlap in the PC to form flat bands. This observation was corrected by Ito et al. [20], who presented a calculation based in a dipolar radiation implemented on the FDTD method to study the PBS, showing a strong distribution of the electromagnetic field on the surface of the rods, near to the resonant frequencies of a single rod under normal incidence for the electromagnetic radiation, that corresponds to the excitation of localized plasmon polariton in the metallic

✉ D. M. Calvo-Velasco  
d.m.calvo-velasco@hotmail.com

<sup>1</sup> Departamento de Física, Universidad del Valle, A. A. 25.360, Cali, Colombia

rod. Esteban Moreno et al. [21], demonstrated that the hypothesis by Ito et al. about the dipolar radiation for the excitation of surface localized modes in the crystal is not enough for another geometry of the rods, being necessary a generalization of the FDTD method using a set of dipoles in the unitary cell. It is important to note that the location shown by Ito et al., as well as the results obtained by Esteban Moreno et al., show that the field at the surface of the metal bars is distributed satisfying any of the symmetries of the metal cross section, also they show that the PBS for the circular cross section has bands with low dispersion below the surface plasmon frequency (SPF). These flat bands are distributed around frequencies which correspond to the resonant modes of the metal rods. Now that Esteban Moreno et al. also presents the study of a PC formed by bars with triangular cross section, showing the existence of flat bands above and below the SPF, demonstrating that the flat bands are distributed around the resonant modes of the rods, but the bands distribution above the SPF depends strongly on the geometry of the cross section of the rods.

In this work we study 2D PCs formed by a square arrangement of rectangular metallic rods without absorption embedded in air. Using the RPWM method we calculate the PBS and some distributions of  $|H_z|^2$  and  $|E|^2$  in the unitary cell of the crystal. In a first case we consider a PC formed of square metallic rods, in order to understand how the PBS depends on the metal plasma frequency. Secondly we consider a PC formed by rectangular metallic rods in air. Also, we modify the rod geometry varying a side of the rods, and show the dependence of the PBS on the size of the rods. Also we present the field distribution which help us to understand how the formation of localized plasmons occurs in these systems.

## 2 Theoretical framework

In this section we present the revised plane wave method (RPWM), [22], for the calculation of the photonic band structure (PBS) of a photonic crystal (PC). We consider, in a general case, a square lattice of parallel rectangular rods made of metallic material with dielectric function  $\epsilon_m$  surrounded by air, whose axes are parallel to  $z$  direction as presented in Fig. 1.

The Maxwell equations to describe the behavior of the electromagnetic radiation in a medium without free charges and currents are:

$$\nabla \times \vec{E} = -\frac{1}{c} \frac{\partial \vec{B}}{\partial t}, \tag{1}$$

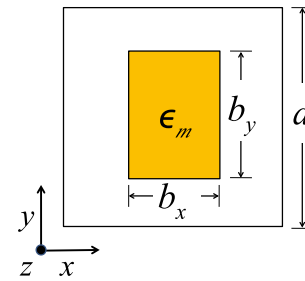


**Fig. 1** Unitary cell representation of a square lattice of rectangular rods of a metallic material with dielectric function  $\epsilon_m$ , immersed in air.  $a$  is the lattice parameter,  $b_x$  and  $b_y$  are the side sizes of the rod

$$\nabla \times \vec{H} = \frac{1}{c} \frac{\partial \vec{D}}{\partial t}, \tag{2}$$

$$\nabla \cdot \vec{H} = 0, \tag{3}$$

$$\nabla \cdot \vec{D} = 0. \tag{4}$$

For linear and isotropic materials, and considering monochromatic waves, we can write

$$\vec{D}(\vec{r}, t) = \epsilon(\vec{r}) \vec{E}(\vec{r}) e^{-i\omega t}, \tag{5}$$

$$\vec{H}(\vec{r}, t) = \vec{H}(\vec{r}) e^{-i\omega t}, \tag{6}$$

where

$$\epsilon(\vec{r}) = 1 + (\epsilon_m - 1)S(\vec{r}), \tag{7}$$

here  $S$  is a function that is 1 in the rods and 0 in the other case. Taking in mind a periodic system in the  $X - Y$  plane,  $\epsilon(\vec{r} + \vec{R}) = \epsilon(\vec{r})$ , with

$$\vec{R} = m \cdot \vec{a}_x + n \cdot \vec{a}_y, \tag{8}$$

and

$$\vec{G} = m \cdot \vec{b}_x + n \cdot \vec{b}_y, \tag{9}$$

the translation vectors in the real and reciprocal space, respectively, related by  $\vec{a}_i \cdot \vec{b}_j = 2\pi\delta_{i,j}$ , we can write for the electric and magnetic fields

$$\vec{E}(\vec{r}) = \sum_G \vec{E}_G e^{i(k+G)\cdot r}, \tag{10}$$

$$\vec{H}(\vec{r}) = \sum_G \vec{H}_G e^{i(k+G)\cdot r}. \tag{11}$$

If the electromagnetic radiation is TE polarized, ( $\vec{H} = (0, 0, H_z)$ ,  $\vec{E} = (E_x, E_y, 0)$ ), the Maxwell equations 1 and 2 take the form

$$\frac{\partial H_z}{\partial y} = -i \frac{\omega}{c} \epsilon E_x, \tag{12}$$

$$\frac{\partial H_z}{\partial x} = i \frac{\omega}{c} \epsilon E_y, \tag{13}$$

$$\frac{\partial E_y}{\partial x} - \frac{\partial E_x}{\partial y} = i \frac{\omega}{c} H_z. \tag{14}$$

Replacing Eqs. 10, 11 in Eqs.12–14 and taking  $N$  terms for the expansion of the fields we obtain

$$(k_y + [[G_y]])[H_z] = -k_0[[\epsilon_{xx}]] [E_x], \tag{15}$$

$$(k_x + [[G_x]])[H_z] = k_0[[\epsilon_{yy}]] [E_y], \tag{16}$$

$$(k_x + [[G_x]])[E_y] - (k_y + [[G_y]])[E_x] = k_0[H_z], \tag{17}$$

where  $k_0 = \frac{\omega}{c}$ , and  $[[G_{x(y)}}]_{G,G'} = G_{x(y)} \delta_{G,G'}$ , are diagonal matrices of order  $N$ .  $[E_x]$ ,  $[E_y]$  and  $[H_z]$  are column vectors of order  $N$  constructed by the coefficients in Eqs. 10 and 11.

The matrices  $[[\epsilon_{xx}]]$ ,  $[[\epsilon_{yy}]]$  are constructed following the Li’s rules for the product of two periodic funtions, [23, 24], in our case

$$[[\epsilon_{xx}]]_{mn,m'n'} = \frac{1}{a} \int_{-a/2}^{a/2} [[A_x^{-1}]]_{m,m'} e^{-i(n-n')g_y y} dy, \tag{18}$$

$$[[A_x]]_{m,m'} = \frac{1}{a} \int_{-a/2}^{a/2} \frac{1}{\epsilon} e^{-i(m-m')g_x x} dx, \tag{19}$$

where  $g_i = \left| \vec{b}_i \right|$  are the elementary translation vectors of the reciprocal lattice. The coefficients of the matrix are relating the term  $\vec{G} = m\vec{b}_x + n\vec{b}_y$  with  $\vec{G}' = m'\vec{b}_x + n'\vec{b}_y$ . A similar construction follows for  $[[\epsilon_{yy}]]$ .

Considering propagation of the radiation in the  $\Gamma - X$  direction ( $k_y = 0$ ) and combining Eqs. 15, 16 and 17, we obtain

$$k_x \begin{bmatrix} [E_y] \\ [H_z] \end{bmatrix} = \frac{1}{k_0} M \begin{bmatrix} [E_y] \\ [H_z] \end{bmatrix} \tag{20}$$

with

$$M = \begin{bmatrix} -k_0[[G_x]] & k_0^2 - [[G_y]][[\epsilon_{xx}]]^{-1}[[G_y]] \\ k_0^2[[\epsilon_{yy}]] & -k_0[[G_x]] \end{bmatrix}. \tag{21}$$

The PBS is obtained solving the eigen values of equation 20.

### 3 Results

#### 3.1 Square rods

By means of Eq. 20, we calculate the PBS of a 2D square PC made of square rods of metal embedded in air for three values of plasma frequency, which in practice

corresponds to different metals. We consider squares rods with  $b_x = b_y = b = 0.25a$ , where  $b$  is the length of the square side and  $a$  is the lattice parameter, as shown in Fig. 1. The dielectric function for the rods is assumed as [25]

$$\epsilon_m = 1 - \frac{\omega_p^2}{\omega^2}, \tag{22}$$

where  $\omega_p$  is the plasma frequency.

In Fig. 2, we observe the PBS characterized with flat bands localized below  $\omega_p$ , behavior that was just reported by Ito et al. [20], due to the characteristic resonance frequencies associated with the existence of surface plasmons on the rod surface. Also, we found that for higher values of the  $\omega_p$ , not only flat bands, but also new dispersive bands appear above the  $\omega_p$ .

In Fig. 3, we present some distributions of  $|H_z|^2$  and  $|E|^2$  in the unitary cell for  $\omega_p a / 2\pi c = 1.0$ . For low frequencies and in the dispersive band, Fig. 3a, we observe that  $|H_z|^2$  and  $|E|^2$  are distributed outside the rod, due to the large negative value of  $\epsilon_m$ , and  $|E|^2$  presents a strong concentration close to the corners of the rod, related with the movement of charge on the surface of the rod, but localized in their corners. On the other side Fig. 3b, c present the field distribution for higher and lower frequencies close to the SPF for bands with low dispersion, showing their strong localization in the rod sides, as a signature of the existence of localized surface plasmons. For frequencies below and above to  $\omega_p$ , Fig. 3d, e present a similar  $|H_z|^2$  distribution in the unitary cell, taking its high values in the inter-rod space and in the rod corners, but this is not the case for the  $|E|^2$  distribution, where for frequencies below  $\omega_p$  the electric field is concentrated into the rod, due to the low absolute value of its refractive index, while for frequencies above  $\omega_p$  the electric field is still distributed inside the rod, but also with a strong presence in the air region. In this case, both materials present a positive refractive index, but the metal has the lower one, which makes the radiation to concentrate inside the rod.

#### 3.2 Rectangular rods

In Fig. 4, we present the PBS for 2D square PC made of rectangular metallic rods embedded in air for different geometries, considering  $\omega_p a / 2\pi c = 1.0$ . We observe that by increasing  $b_y$  from  $0.25a$  to  $0.8a$  leaving  $b_x = 0.25a$  the PBS splits the band distribution. The reason for the change in the PBS is related with the rods geometry, and consequently with the filling fraction, somehow influenced by the plasmon resonant modes on the rod surface. Also we observe the modification of the first band with  $b_y$  variation

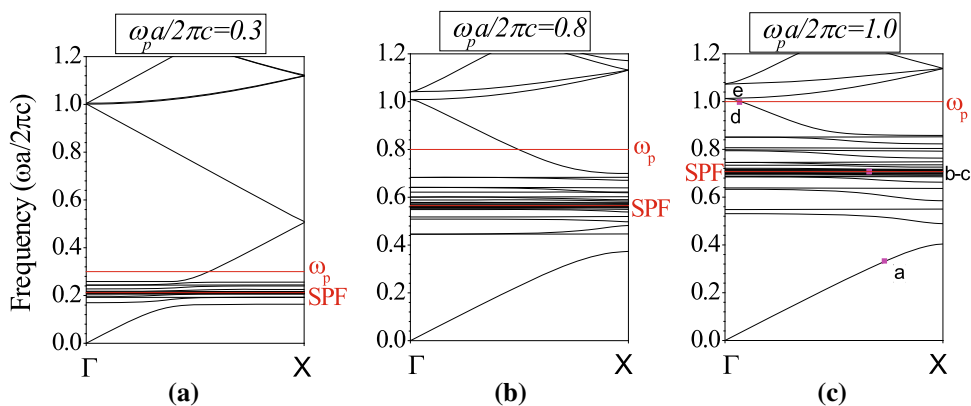


**Fig. 2** Photonic band structure for TE polarization in the  $\Gamma - X$  direction of a square lattice of square metallic rods in air with  $b/a = 0.25$ , being  $a$  the lattice parameter and  $b$  the side size of the square rod. The value of plasma frequency is: **a**  $\omega_p a/2\pi c = 0.3$ ,

**b**  $\omega_p a/2\pi c = 0.8$ , **c**  $\omega_p a/2\pi c = 1.0$ . Red lines show the  $\omega_p$  frequency and the value of the SPF. The purple marked squares *a-e* in **c** are to display  $|H_z|^2$  and  $|E|^2$  as it is presented in Fig. 3

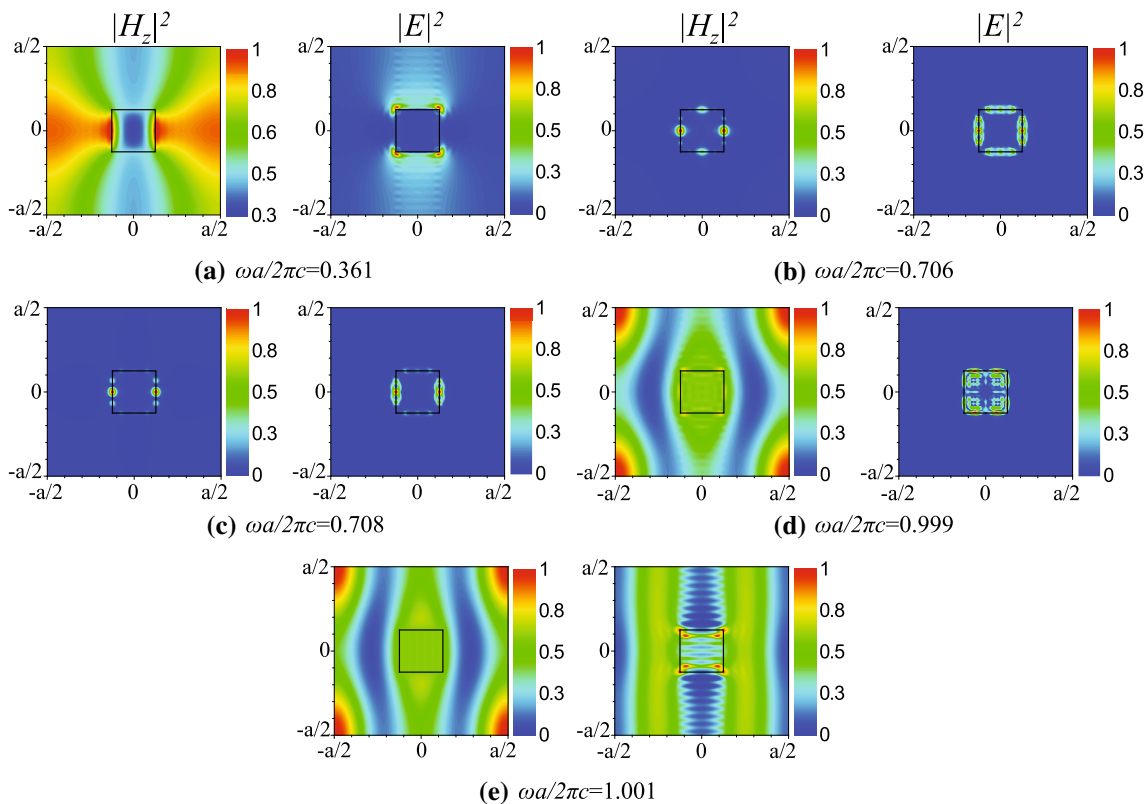


**Fig. 3** Some  $|H_z|^2$  and  $|E|^2$  distributions in the unitary cell of a PC made of rectangular metallic rods with sides  $b_x = 0.25a$ ,  $b_y = 0.25a$  and  $\omega_p a/2\pi c = 1.0$  in air. The intensity distribution is in arbitrary units

until its disappearance in the 1D PC limit, that is for  $b_y = 1.0$  presented in Fig. 4c. In this case the first gap is due to the existence of an effective plasma frequency, that shields the propagation of the radiation in this structure, related with the filling fraction of the slab in the unitary cell.

Figure 5 displays some distributions of  $|H_z|^2$  and  $|E|^2$  in the unitary cell for frequencies depicted in Fig. 4b for  $b_x =$

$0.25a$  and  $b_y = 0.80a$ . We observe for a low frequency, Fig. 5a,  $|H_z|^2 - |E|^2$  are mainly distributed outside the rod, due to the high negative value of  $\epsilon_m$ . In the case of  $|E|^2$  distribution, high localization occurs in the inter-rod space in the  $y$  direction. In a band with low dispersion, Fig. 5b,  $|H_z|^2 - |E|^2$  distributions present strong localization in the

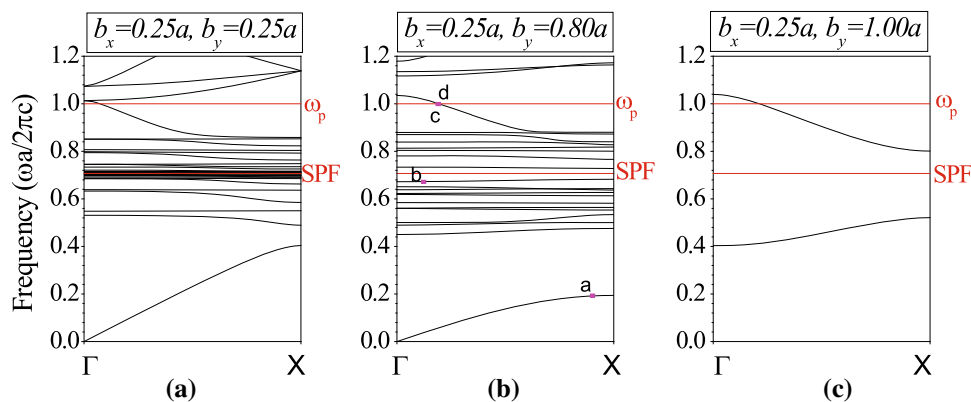


**Fig. 4** Photonic band structure for TE polarization in the  $\Gamma - X$  direction of a square lattice of rectangular metallic rods in air. The value of plasma frequency is  $\omega_p a / 2\pi c = 1.0$ . The red line shows the value of plasma frequency. Rectangle sides are  $b_x = 0.25a$ :

**a**  $b_y = 0.25a$ , **b**  $b_y = 0.80a$ , **c**  $b_y = 1.00a$ . Red lines show the  $\omega_p$  frequency and the value of the SPF. The purple marked squares  $a - d$  in **b** are to display  $|H_z|^2$  and  $|E|^2$  as it is presented in Fig. 5

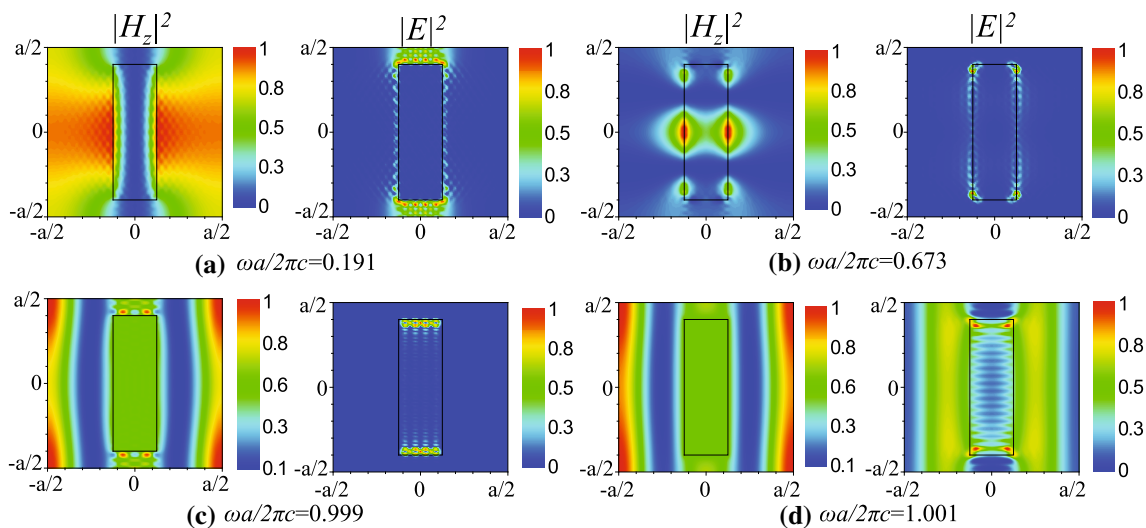


**Fig. 5** Some  $|H_z|^2$  and  $|E|^2$  distributions in the unitary cell of a PC made of rectangular metallic rods with sides  $b_x = 0.25a$ ,  $b_y = 0.80a$  and  $\omega_p a / 2\pi c = 1.0$  in air. The intensity distribution is in arbitrary units

large sides of the rod, evidence of surface plasmons, with a high concentration of  $|E|^2$  in the rod corners, behavior just presented and discussed above in Fig. 3. For a frequency below  $\omega_p$ , Fig. 5c, the  $|E|^2$  distribution mainly occurs inside the rod. As was mentioned above in Fig. 3d, in this situation the localization is due to the low absolute value of the refractive index of the metal compared with the air, which drives the radiation to enter in the rod region. Meanwhile for a frequency above  $\omega_p$ , Fig. 5d, we observe that  $|E|^2$  is localized inside and outside the rod, taking high values close to the rod corners. A similar result was previously presented and discussed in Fig. 3e for the square case. A similar  $|H_z|^2$  distribution is observed for frequencies below and above  $\omega_p$ . It is important to mention that the

high localization below  $\omega_p$  is reinforced by the proximity of the rectangular rod in the  $y$  direction.

### 4 Conclusions

Previous researches to this work have shown that PCs formed with dispersive materials have exciting phenomenology that improve the light propagation control thanks to the existences of plasmon resonances in the surface of the materials. In this work, we used the RPWM to calculate the PBS in the  $\Gamma - X$  direction of a 2D square PC made of rectangular metallic rods embedded in air for the TE polarization. In the case of square metallic rods, we

found that the PBS of the PC is reallocated and shifted to lower or higher frequencies depending significantly on  $\omega_p$ . Also, the PBS presents bands with low dispersion below  $\omega_p$ , distributed around the SPF. For frequencies close to the SPF the distributions show a strong localization of the field in the surface of the rods. For frequencies between the SPF and  $\omega_p$  the decrease in the  $|\epsilon_m|$  values is related with the increase of  $|E|^2$  localization in the rods region, even for frequencies close to  $\omega_p$ . In the case of rectangular metallic rods, the PBS shows a modification of low dispersion bands depending on the length of the rod sides. For the chosen frequencies our results present for  $|E|^2$  a high concentration close to the rod corners. On the other hand,  $|H_z|^2$  shows the formation of surface plasmons for frequencies in bands with low dispersion, behavior that is also observed for  $|E|^2$ . For frequencies below and above, but close to  $\omega_p$ ,  $|E|^2$  shows a high presence into the rod region, just like in the case of square rods.

**Acknowledgments** D. M. Calvo-Velasco would like to thank the Colombian Scientific Agency COLCIENCIAS for partial financial support of this work.

## References

1. J.D. Joannopoulos, S.G. Johnson, J.N. Winn, R.D. Meade, *Photonic Crystals: Molding the Flow of Light* (Princeton University Press, Princeton, 2008)
2. K. Sakoda, *Optical Properties of Photonic Crystals*, 2nd edn. (Springer, Berlin, 2005)
3. S.A. Ramakrishna, T.M. Grzegorzczak, *Physics and Applications of Negative Refractive Index Materials* (Taylor & Francis Group, Bellingham, 2009)
4. N. Engheta, R.W. Ziolkowski, *Metamaterials: Physics and Engineering Explorations* (IEEE Press, Wiley-Interscience, Hoboken, 2006)
5. S.B. Cavalcanti, M. de Dios-Leyva, E. Reyes-Gomez, L.E. Oliveira, Band structure and band-gap control in photonic superlattices. *Phys. Rev. B* **74**, 153102 (2006)
6. Luz E. González, N. Porrás Montenegro, Pressure, temperature and plasma frequency effects on the band structure of a 1D semiconductor photonic crystal. *Phys. E* **44**, 773 (2012)
7. B.F. Díaz-Valencia, J.M. Calero, Photonic band gaps of a two-dimensional square lattice composed by superconducting hollow rods. *Phys. C* **505**, 74 (2014)
8. J. López, Luz E. González, M.F. Quiñónez, M.E. Gómez, N. Porrás-Montenegro, G. Zambrano, Magnetic field role on the structure and optical response of photonic crystals based on ferrofluids containing  $Co_{0.25}Zn_{0.75}Fe_2O_4$  nanoparticles. *J. Appl. Phys.* **115**, 193502 (2014)
9. K. Sakoda, Electromagnetic eigenmodes of a three-dimensional photonic fractal. *Phys. Rev. B* **72**, 184201 (2005)
10. J.R. Mejía, N. Porrás-Montenegro, E. Reyes, S.B. Cavalcanti, L.E. Oliveira, Plasmon polaritons in 1D Cantor-like fractal photonic superlattices containing a left-handed material. *Europhys. Lett.* **95**, 24004 (2011)
11. Paul V. Braun, S.A. Rinne, F. García-Santamaría, Introducing defects in 3D photonic crystals: state of the art. *Adv. Mater.* **18**, 2665–2678 (2006)
12. C.-J. Wu, Z.-H. Wang, Properties of defect modes in one-dimensional photonic crystals. *Prog. Electromagn. Res.* **103**, 169–184 (2010)
13. V. Veselago, L. Braginsky, V. Shklover, C. Hafner, Negative refractive index materials. *J. Comput. Theor. Nanosci.* **3**, 1 (2006)
14. V. Kuzmiak, A.A. Maradudin, F. Pincemin, Photonic band structures of two-dimensional systems containing metallic components. *Phys. Rev. B* **50**, 16835 (1994)
15. V. Kuzmiak, A.A. Maradudin, A.R. McGurn, Photonic band structures of two-dimensional systems fabricated from rods of a cubic polar crystal. *Phys. Rev. B* **55**, 4298 (1997)
16. V. Kuzmiak, A.A. Maradudin, Distribution of electromagnetic field and group velocities in two-dimensional periodic systems with dissipative metallic components. *Phys. Rev. B* **58**, 7230 (1998)
17. K. Sakoda, N. Kawai, T. Ito, A. Chutinan, S. Noda, T. Mitsuyu, K. Hirao, Photonic bands of metallic systems. I. Principle of calculation and accuracy. *Phys. Rev. B* **64**, 045116 (2001)
18. K.C. Huang, P. Bienstman, J.D. Joannopoulos, K.A. Nelson, S. Fan, Phonon-polariton excitations in photonic crystals. *Phys. Rev. B* **68**, 075209 (2003)
19. S. Maier, *Plasmonics: Fundamentals and Applications* (Springer, Berlin, 2007)
20. T. Ito, K. Sakoda, Photonic bands of metallic systems. II. Features of surface plasmon polaritons. *Phys. Rev. B* **64**, 045117 (2001)
21. E. Moreno, D. Erni, C. Hafner, Band structure computations of metallic photonic crystals with the multiple multipole method. *Phys. Rev. B* **65**, 155120 (2002)
22. S. Shi, C. Chen, D.W. Prather, Revised plane wave method for dispersive material and its application to band structure calculations of photonic crystal slabs. *Appl. Phys. Lett.* **86**, 043104 (2005)
23. L. Li, Use of Fourier series in the analysis of discontinuous periodic structures. *J. Opt. Soc. Am. A* **13**, 1870 (1996)
24. P. Lalanne, Effective properties and band structure of lamellar subwavelength crystals: plane-wave method revisited. *Phys. Rev. B* **58**, 9801 (1998)
25. C. Kittell, *Introduction to Solid States Physics*, 7th edn. (Wiley, New York, 1966)